

ilar impurity combined resonance data in InSb. The first (Ref. 4) invoked an electron-TO-phonon interaction in addition to the usual electron-LO-phonon interaction to explain the *two* "polaron anomalies" observed in the combined resonance spectra; the second (Ref. 7) asserted that only the electron-LO-phonon interaction was important, and the upper "polaron anomaly" was due to coupling to an impurity excited state. Of crucial importance in the interpretation of this data is a knowledge of the impurity spin energy of the lowest Landau level. Figure 4 shows the combined resonance data of Ref. 7 with the  $L=0$  spin energies obtained from the EDE-ESR measurements subtracted. The shaded bands labeled LO and TO cover the ranges of the values of these phonon en-

ergies quoted in the literature (see Ref. 7). The impurity spin energy will be smaller than the measured free carrier spin energy due to the effects of nonparabolicity on the impurity binding energies. This will raise the experimental points even higher. It is obvious that the lowest "anomaly" occurs at  $\omega_{LO}$  and *not*  $\omega_{TO}$ . Hence the interpretation in terms of LO-phonon coupling alone is apparently correct, and the impurity electron-TO-phonon coupling must be much weaker.

#### ACKNOWLEDGMENTS

The authors are indebted to Dr. E. J. Johnson for communication of his calculated spin energies. Thanks are also due Dr. G. A. Prinz for experimental assistance and discussions.

<sup>1</sup>B. D. McCombe, R. J. Wagner, and G. A. Prinz, *Phys. Rev. Letters* **25**, 87 (1970).

<sup>2</sup>R. L. Bell, *Phys. Rev. Letters* **9**, 52 (1962).

<sup>3</sup>B. D. McCombe, *Phys. Rev.* **181**, 1206 (1969).

<sup>4</sup>D. H. Dickey and D. M. Larsen, *Phys. Rev. Letters* **20**, 65 (1968).

<sup>5</sup>C. R. Pidgeon, D. L. Mitchell, and R. N. Brown, *Phys. Rev.* **154**, 737 (1967).

<sup>6</sup>E. J. Johnson and D. H. Dickey, *Phys. Rev. B* **1**, 2676 (1970).

<sup>7</sup>B. D. McCombe and R. Kaplan, *Phys. Rev. Letters* **21**, 756 (1968).

<sup>8</sup>V. I. Sheka, *Fiz. Tverd. Tela* **6**, 3099 (1964) [*Sov. Phys. Solid State* **6**, 2470 (1965)].

<sup>9</sup>G. A. Prinz and R. J. Wagner, *Phys. Letters* **30A**, 520 (1969).

<sup>10</sup>R. Kaplan, *Appl. Opt.* **6**, 685 (1967).

<sup>11</sup>R. A. Isaacson, *Phys. Rev.* **169**, 312 (1968).

<sup>12</sup>R. Bowers and Y. Yafet, *Phys. Rev.* **115**, 1165 (1959).

<sup>13</sup>S. H. Groves, C. R. Pidgeon, A. W. Ewald, and R. J. Wagner, *J. Phys. Chem. Solids* **31**, 2031 (1970).

<sup>14</sup>B. D. McCombe, *Solid State Commun.* **6**, 533 (1968).

<sup>15</sup>B. D. McCombe, R. J. Wagner, and G. A. Prinz, *Solid State Commun.* **7**, 1381 (1969).

## Low-Temperature Grüneisen Parameters for Silicon and Aluminum<sup>†</sup>

W. B. Gauster

*Sandia Laboratories, Albuquerque, New Mexico 87115*

(Received 29 March 1971)

From measurements of the inertial thermoelastic stress produced by pulse heating a portion of a sample, the Grüneisen parameters of silicon and aluminum as a function of temperature were obtained directly between 5 and 290°K. Pulses of 1.5-MeV average-energy electrons, lasting approximately 40 nsec, were used as the heating agent, and the stresses were recorded with a quartz gauge bonded to the back face of the sample. For silicon, the low-temperature stress measurements indicated a limit of the Grüneisen parameter of about 0.2, which is lower than the value calculated from thermal-expansion data but in agreement with that calculated from pressure derivatives of elastic constants. For aluminum (6061 alloy-97% Al), the low-temperature limit of the lattice Grüneisen parameter was found to be 1.7 and the electronic contribution was estimated to be 1.7 as well, agreeing within experimental uncertainty (approximately 25%) with published values based on thermal-expansion measurements on pure aluminum.

### I. INTRODUCTION

Recently, precise measurements of elastic-stress pulses resulting from the heating of solid samples by brief bursts of MeV electrons have been related to the Grüneisen parameters of the absorbing materials.<sup>1-4</sup> Absolute determinations of room-tem-

perature Grüneisen parameters were accomplished by combining the elastic displacement measurements with electron-beam dosimetry.<sup>3,4</sup> Related free-carrier effects in semiconductors have been analyzed.<sup>5</sup>

The purpose of this paper is to report the measurement of thermoelastic stresses to determine

directly the variation of the Grüneisen parameter between 5 and 290 °K and to present results for silicon and aluminum.

*Grüneisen parameters.* In the quasiharmonic approximation, a solid is represented by a collection of harmonic oscillators whose frequencies are functions of the volume. These dependences are expressed by the mode Grüneisen parameters  $\gamma_i = -(\partial \ln \omega_i / \partial \ln V)_T$  where  $\omega_i$  is the frequency of the  $i$ th lattice mode,  $V$  is the volume, and  $T$  is the temperature.

An average of the mode parameters can be defined by

$$\gamma(T) = \frac{\sum_i \gamma_i c_i}{\sum_i c_i}, \quad (1)$$

where the weighting factors  $c_i$  are the contributions to the specific heat at constant volume,  $C_V$ , from the respective modes.  $\gamma$  is a function of temperature because the vibrational modes contribute variously to the specific heat at different temperatures.

Through the expression for the free energy of the system,  $\gamma$  can be written in terms of macroscopic observables. Specifically,

$$\begin{aligned} \gamma &= V \frac{\partial^2 F}{\partial V \partial T} / T \frac{\partial^2 F}{\partial T^2} \\ &= \beta B_T V / C_V, \end{aligned} \quad (2)$$

where  $F$  is the free energy,  $\beta$  the volume coefficient of thermal expansion, and  $B_T$  the isothermal bulk modulus.

Often  $\gamma$  is readily derived from a theoretical model, and a comparison of predicted and experimentally determined Grüneisen parameters is of interest. Moreover, the above formalism can accommodate electronic and magnetic contributions to  $\gamma$ , and it is also instructive to follow the Grüneisen parameter through phase transitions.

At temperatures much below the Debye temperature,  $\gamma$  approaches a limiting value which can be calculated on the basis of the continuum model from pressure derivatives of the elastic constants. Within the validity of the assumptions, that value should agree with the low-temperature limit of expression (2).

*Thermal expansion.* In determining experimentally the terms on the right-hand side of Eq. (2), the problem is encountered that both  $\beta$  and  $C_V$  approach zero at low temperatures. Particularly the thermal-expansion<sup>6</sup> coefficient is difficult to measure, as can be appreciated from the fact that the total length change of a 7-cm-long metal sample between 0 and 6 °K varies between 2 Å for tungsten and 500 Å for lead.<sup>7</sup> For many other materials, the length change is smaller still, and it is the derivative of this quantity that must be determined. It is not surprising, then, that the early determinations of the low-temperature values of the lattice  $\gamma$  through

Eq. (2) for aluminum varied between 1.7<sup>8</sup> and 3.63 ± 0.23<sup>9</sup> at about 0.05 the Debye temperature, and that discrepancies were observed between the limiting values of  $\gamma$  from Eq. (2) and that calculated from third-order elastic constant data for silicon.<sup>10,11</sup>

*Thermoelastic stress.* There is, however, a third and direct method of determining  $\gamma$ . Equation (2) can be written

$$\gamma = V \left( \frac{\partial P}{\partial T} \right)_V / C_V = V \left( \frac{\partial P}{\partial E} \right)_V, \quad (3)$$

where  $E$  is the internal energy. Thus the pressure change caused by a change of internal energy at constant volume provides a direct measure of the Grüneisen parameter.

Experimentally, the necessary conditions can be achieved by pulse heating a sample internally at a rate sufficiently high for the material to remain inertially clamped during the process. A stress pulse then propagates out of the heated region and can be measured at the rear surface of the sample. Its shape is determined by the energy deposition profile and its magnitude is related to the Grüneisen parameter through the absorbed energy density.

The internal heating can be accomplished with a burst of MeV electrons. Measurements, with a quartz gauge, of stress pulses produced in this way in several materials were first related to relative room-temperature Grüneisen parameters by Graham and Hutchison.<sup>1</sup> Similar experiments, using a laser interferometer to record rear surface motion, were reported by Oswald *et al.*<sup>2</sup> Recently, such measurements were combined with beam dosimetry to obtain absolute Grüneisen parameter values at room temperature.<sup>3,4</sup>

Measurements of peak stresses produced as a function of sample temperature by electron pulses of given total energy yield directly the temperature dependence of the Grüneisen parameter. The advantage of this technique is that it involves only one measurement, and that the measured quantity remains finite at low temperatures. To preserve temperature resolution at low temperatures, the amount of heat supplied to the sample per pulse must be kept small.

## II. THERMOELASTIC STRESS PRODUCTION

The problem of stress production due to internal heat addition has been investigated by Zaker<sup>12</sup> for a linear thermoelastic solid. He derived the equation of motion for the case of uniaxial strain in a slab with stress-free surfaces, heated by the absorption of power with a specified space and time variation. In the case of interest here, the thermal conductivity is negligible and the uncoupled wave equation is considered:

$$\sigma_{tt} - \alpha^2 \sigma_{xx} = \rho \gamma P_t, \quad (4)$$

where  $\sigma$  is the stress component perpendicular to the irradiated slab surface,  $a$  is the adiabatic dilatational sound velocity,  $\rho$  is the mass density, and  $P$  is the power deposited per unit mass.  $\gamma$  is the Grüneisen parameter; the subscripts indicate differentiation with respect to time  $t$  and distance  $x$  perpendicular to the irradiated surface into the sample. In the experiments, the total sample thickness was greater than the heated region, but the analysis does not require that condition.

Zaker writes the solution of (4) as a pair of line integrals over the characteristics in the  $x$ - $t$  plane, extending from  $(x, t)$  to the abscissa. To account for the sign reversal of stresses on reflection from the free slab surfaces, a system of image slabs is constructed and a power-source distribution of alternating signs is specified in the image slabs. The correct sign for the source and image sources must be used over the appropriate portions of the line integrals:

$$\sigma(x, t) = \frac{1}{2} \rho \gamma \int_0^t \{ P[x - a(t - \tau), a\tau] + P[x + a(t - \tau), a\tau] \} d\tau. \quad (5)$$

If  $E(x)$  is the energy deposition profile in the absorber, a rectangular power pulse of duration  $\tau_0$  is represented by

$$P(x, t) = \begin{cases} E(x)/\tau_0, & 0 \leq t \leq \tau_0 \\ 0, & t > \tau_0. \end{cases} \quad (6)$$

The compressive stress measured by an acoustically matched transducer bonded to the rear surface ( $x=L$ ) of the sample is then

$$\sigma(L, t) = (\rho \gamma / 2a\tau_0) \int_{L-at}^{L-a(t-\tau_0)} E(y) dy. \quad (7)$$

In the limit as  $\tau_0$  (the deposition time) becomes negligibly small with respect to the acoustic transit time through the deposition region, Eq. (7) reduces to

$$\sigma(L, t) = \frac{1}{2} \rho \gamma E(L - at). \quad (8)$$

Owing to the boundary conditions, the compressive stress of Eqs. (7) and (8) is followed immediately by a tensile pulse of equal magnitude.

In the experiments, the sample face was irradiated uniformly and the sample radius was always at least twice the sample thickness, so that the one-dimensional analysis would apply. The effect of heating rate [Eq. (7)] has been investigated experimentally,<sup>13</sup> and the analysis was found to agree with measurements. In the present experiments, the ratio of deposition time to acoustic relaxation time was sufficiently small for Eq. (8) to be used with only a slight (5%) error resulting in the calculated Grüneisen parameter. If the data are normalized to the correct room-temperature value, the tem-

perature dependence of  $\gamma$  is of course obtained from (8) with no error introduced due to the assumption of an infinite heating rate.

### III. ELECTRONIC VOLUME EFFECT

As discussed in Ref. 5, the stress produced by a brief burst of ionizing radiation in a semiconductor is due not only to the heating of the lattice but also to the excitation of electron-hole pairs. Associated with the changed population of the energy levels is a new equilibrium volume, and thus a contribution to the inertial stress propagating out of the region of absorption. In highly doped semiconductors, however, the lifetimes of the excited carriers can be very brief, and the energy is transferred to the lattice in a time shorter than the duration of a 40-nsec exciting pulse. It was shown in Ref. 5 that, while the stress measured in intrinsic semiconductors depended on the lifetimes (and thus the densities) of electron-hole pairs produced, in highly doped materials the stress was independent of dose and just proportional to the thermodynamic Grüneisen parameter.

When a semiconductor is irradiated, the energy of the ionizing radiation is transferred in part to the lattice through phonon collisions and the remainder is used up in producing electron-hole pairs by impact ionization. As long as the energy of the incoming radiation is much greater than the band gap, the total energy  $\epsilon$  used up in producing one carrier pair is independent, at least to a first approximation, of the mass, charge, and velocity of the incident particle.<sup>14</sup> There is, however, a dependence of the value of  $\epsilon$  on the bandgap. Shockley<sup>15</sup> gives the relation

$$\epsilon = 2.2E_g + \nu E_R, \quad (9)$$

where  $E_g$  is the bandgap energy,  $E_R$  is the optical phonon energy, and  $\nu$  is the ratio of the mean free path between ionizing collisions to that between phonon collisions.

Both the bandgap and the mean free path between ionizing collisions are temperature dependent. Measurements of  $\epsilon$  for 1-MeV electrons incident on silicon have been made from 300°K down to 20°K by Emery and Rabson.<sup>16</sup> They combined Shockley's equation with an expression for the mean free time between ionizing collisions due to Beattie and Landsford.<sup>17</sup> The resulting expression for  $\epsilon$  as a function of temperature contains two constants, which were evaluated by fitting a curve to the data to give

$$\epsilon(T) = 2.2E_g(T) + 1.08E_g^{3/2}(T) e^{11.2E_g(T)/T}. \quad (10)$$

Thus, when the stress produced by electron pulses of constant depth-dose profile  $E(L - at)$  is measured as a function of sample temperature  $T$ , Eq. (8) applies for metals and highly doped semiconductors and can be rewritten

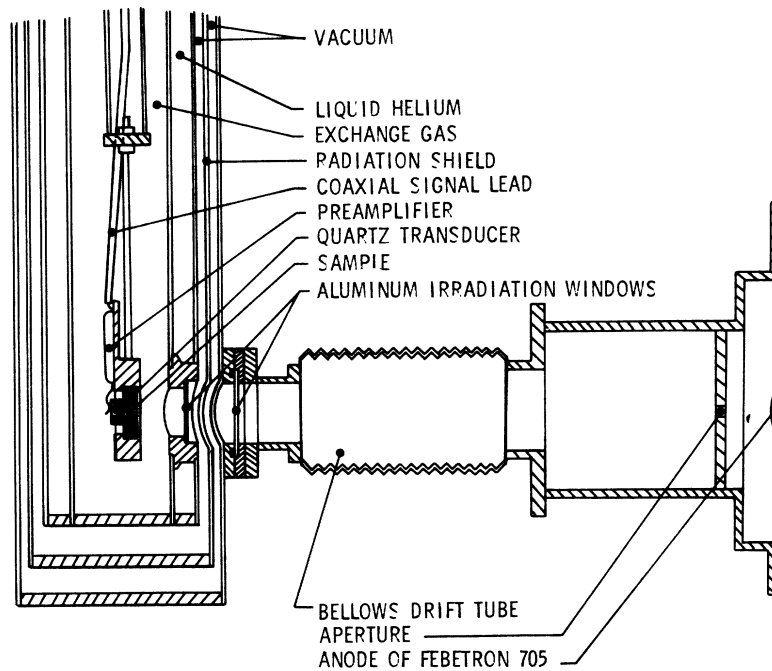


FIG. 1. Experimental arrangement.

$$2\sigma(L, t, T) = \gamma(T)\rho(T)E(L - at). \quad (11)$$

The corresponding expression for semiconductors with carrier lifetimes longer than the duration of the pulse of incident radiation is obtained from Eqs. (9), (18), and (19) of Ref. 5:

$$2\sigma^*(L, t, T) = \{\gamma(T)[1 - E_g(T)/\epsilon(T)] + (dE_g/dP)/K(T)E_g(T)\}\rho(T)E(L - at), \quad (12)$$

where  $K$  is the isothermal compressibility and  $\epsilon(T)$  is given by Eq. (10). By comparison with Eq. (11), the term in brackets in Eq. (12) denotes an "effective" Grüneisen parameter, which includes the electronic volume effect.

#### IV. EXPERIMENT

A diagram of the experimental arrangement is shown in Fig. 1. The source of electrons was a Febetron 705 machine,<sup>18</sup> which supplied pulses of about 40-nsec duration and 1.5-MeV average electron energy. The sample-transducer configuration was the same as in Ref. (5), except that the sample and transducer were mounted in an exchange gas Dewar.<sup>19</sup> The electrons emerged from the anode of the accelerator into an evacuated drift tube and through two thin aluminum irradiation windows into the sample chamber. An aperture in the drift tube reduced the dose incident on the sample.

The sample was mounted on a copper block which contained cartridge heaters as well as platinum and germanium temperature sensors. To bond the quartz transducer to the sample, the best results

were achieved with the adhesive from a cellulose tape.<sup>20</sup> In some runs Dow Corning 200 fluid of 200 000-centistokes viscosity was used to form the bond. The quartz was pressed against the sample by a spring. The two electroded faces of the transducer were connected by a 2-k $\Omega$  resistor (constant to within  $\frac{1}{2}\%$  over the temperature range) and the face bonded to the sample was at ground potential. The voltage across the resistor provided the record of the stress. A field-effect-transistor (FET) preamplifier<sup>21</sup> was mounted directly behind the transducer and drove the 50- $\Omega$  coaxial line leading out of the Dewar through a pulse amplifier to the oscilloscope.

The samples were disks, 2.5 to 3 cm in diam and 0.5 to 0.6 cm thick. The faces were lapped flat to  $\frac{1}{4}\lambda$  sodium light and parallel to 5 parts in  $10^5$ . The aluminum sample was machined from 6061 alloy, consisting of 97% Al. The principal impurities were 1.0% Mg, 0.6% Si, and 0.25% each Cu and Cr. The silicon samples were cut from single-crystal boules, with the faces normal to the [111] direction. Both were  $p$  type, boron doped, one residually doped with a resistivity between  $10^3$  and  $3 \times 10^3 \Omega \text{ cm}$ , the other with a resistivity between  $1.5 \times 10^{-3}$  and  $2.5 \times 10^{-3} \Omega \text{ cm}$ .

The amount of energy supplied to the sample in each electron burst had to be kept low to minimize sample heating, particularly at low temperatures where the specific heat is small. The amount of energy per pulse was made as small as was compatible with an acceptable signal-to-noise ratio, and was kept the same for measurements at all

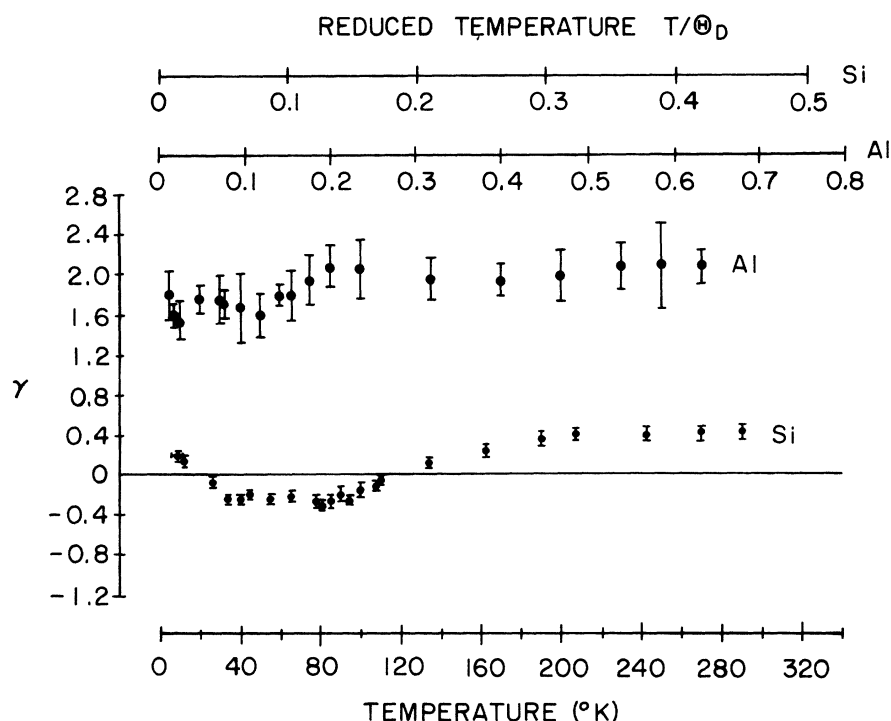


FIG. 2. Grüneisen parameters of silicon and aluminum as functions of sample temperature, determined from measurements of inertial thermoelastic stresses.

temperatures. In this way the measurement uncertainty was constant over the entire temperature range, although the temperature resolution became worse at the lowest temperatures. The peak energy densities in the absorbers were  $1.3 \times 10^{-3}$  J/g, producing peak pressures on the order of 10 mbar.

The temperature rise in the region of peak absorbed energy density can be calculated by integrating under the curve of specific heat vs temperature. For an aluminum<sup>22</sup> sample initially at 5°K, the region of peak energy deposition was heated to about 7°K. The measured stress was proportional to an average of the Grüneisen parameter over that temperature interval. At higher initial temperatures, the resolution rapidly improved. For example, an aluminum sample initially at 10°K was heated to 10.9°K, one at 15 to 15.3°K, etc. For silicon,<sup>23</sup> the region of peak energy density was heated from 5 to almost 12°K, from 10 to almost 13°K, from 15 to 16°K, etc.

It was found that the most reproducible electron-pulse characteristics were obtained if the machine was fired at constant intervals of a least 4 min.

#### V. RESULTS

Although silicon was the material of prime interest in this investigation, measurements were also made on aluminum because of the expected differences in the behavior of the two elements. Figure 2 shows that the Grüneisen parameter of aluminum remained very nearly constant over the

entire temperature range, while that of silicon went through the expected region of negative values. These silicon data are for the highly doped material, in which the electronic volume effect is not observed. The results on the undoped silicon, which did exhibit the electronic volume effect, will be discussed later.

Each point in Fig. 2 represents an average of four to six shots; some points are averages of different runs. Data were retained only from runs that showed no hysteresis (attributable to poor bonding of the transducer to the sample) in cycling the temperature. The error bars represent the root-mean-square deviation of the data points. The stresses at room temperature were normalized to the Grüneisen parameter value of 2.1 determined by Perry<sup>4</sup> for aluminum and to the value 0.43 for silicon.<sup>24</sup>

*Aluminum.* The Grüneisen parameter for aluminum is seen to remain nearly constant as the temperature is lowered, dropping to about 1.7 at 0.05 of the Debye temperature<sup>22</sup>  $\Theta_D = 428$ °K. At 10°K, the electronic contribution to the specific heat is about  $\frac{1}{3}$  of the total, becoming  $\frac{3}{4}$  of the total at 4°K. Using the expression

$$\gamma = (C_l \gamma_l + C_e \gamma_e) / C_v, \quad (13)$$

where the subscripts *l* and *e* indicate the lattice and electronic contributions, respectively, to the specific heat and Grüneisen parameter, and using the specific-heat data of Berg,<sup>22</sup>  $\gamma_e$  is estimated

TABLE I. Compilation of Grüneisen parameters for aluminum.

Technique	Reference	Temperature (°K)	$\gamma_i$	$\gamma_e$
Thermal expansion	Bijl and Pullan <sup>a</sup>	273	2.15	
		35	1.7	
	Huzan, Abbiss, and Jones <sup>b</sup>	100	2.5	
		35	3.1	
		15	4.1 ± 2	
	Fraser and Hollis Hallett <sup>c</sup>	80	2.51	
		25	3.63 ± 0.23	
	White <sup>d</sup>	280	2.35	
		80	2.5	
	Andres <sup>e</sup>	< 20	2.65 ± 0.15	1.8 ± 0.1
		280	2.35	
		< 12	2.3 ± 0.5	2.0 ± 0.5
Critical field	Carr and Swenson <sup>f</sup>			1.34 ± 0.08
	Gross and Olsen <sup>g</sup>			5.65 ± 3
	Harris and Mapother <sup>h</sup>			6.65 ± 3
	Palmy and de Trey <sup>i</sup>			2.6 ± 0.8
Pressure derivative of elastic constants	Schmunk and Smith <sup>j</sup>	> $\Theta_D$	2.56	
		<< $\Theta_D$	2.60	
	Thomas <sup>k</sup>	> $\Theta_D$	2.27	
		<< $\Theta_D$	2.33	
Inertial thermoelastic stress	Oswald <i>et al.</i> <sup>l</sup>	295	2.05	
	Perry <sup>m</sup>	295	2.11 ± 0.2	
	this experiment	80	2.0 ± 0.5	
		20	1.7 ± 0.5	
		5	1.7 ± 0.5	1.7 ± 0.5

<sup>a</sup>Reference 8.<sup>b</sup>E. Huzan, C. P. Abbiss, and G. O. Jones, *Phil. Mag.* **6**, 277 (1961).<sup>c</sup>Reference 9.<sup>d</sup>G. K. White, in *Proceedings of the Eighth International Conference on Low-Temperature Physics, London, 1962*, edited by R. O. Davies (Butterworths, London, 1963), p. 394.<sup>e</sup>Reference 7.<sup>f</sup>R. H. Carr and C. A. Swenson, *Cryogenics* **4**, 76 (1964),

quoted in (h).

<sup>g</sup>D. Gross and J. L. Olsen, *Cryogenics* **1**, 91 (1960).<sup>h</sup>E. P. Harris and D. E. Mapother, *Phys. Rev.* **165**, 522 (1968).<sup>i</sup>C. Palmy and P. de Trey (unpublished), quoted in Ref. 26.<sup>j</sup>R. E. Schmunk and C. S. Smith, *J. Phys. Chem. Solids* **9**, 100 (1959).<sup>k</sup>J. F. Thomas, Jr., *Phys. Rev.* **175**, 955 (1968).<sup>l</sup>Reference 3.<sup>m</sup>Reference 4.

from Fig. 2 to be about 1.7 also.

Comparison can be made to a number of investigations found in the literature. Table I is a compilation of values obtained by four different techniques. All the results are for "pure" aluminum except those of Perry and of the present experiment, which are for 6061 alloy. The relatively slight alloying should not significantly affect the results,<sup>25</sup> and the room-temperature results of Oswald *et al.* for single-crystal aluminum and of Perry for 6061 alloy agree well.

The room-temperature thermoelastic-stress measurements yielded values of  $\gamma_i$  10–15% lower than the thermal-expansion measurements of White and of Andres. The present measurements were normalized to the room-temperature thermoelastic results and show, within experimental accuracy, the same near constancy with decreasing temperature displayed by  $\gamma$  calculated from the measurements of White and of Andres. The rise of  $\gamma_i$  at low temperatures calculated from the earlier thermal-ex-

pansion results was not observed. The elastic-constant measurements, too, predict  $\gamma_i$  to be nearly the same at high and at low temperatures, and the accuracy of the present experiments was not sufficient to allow a conclusion about the small change predicted from the elastic-constant data.

The electronic contribution to the Grüneisen parameter is simply the logarithmic volume derivative of the electronic specific-heat constant, and it can be calculated from values of the critical field of superconducting aluminum as a function of temperature and pressure.<sup>26</sup> The calculation involves an extrapolation, and inconsistencies between thermal-expansion and critical-field determinations have been observed for a number of materials. Of the values for aluminum shown in Table I, the most recent data (Palmy and de Trey) actually show fair agreement with thermal-expansion and thermal-stress measurements.

The stress records obtained in the present experiments indicate the change of the acoustic tran-

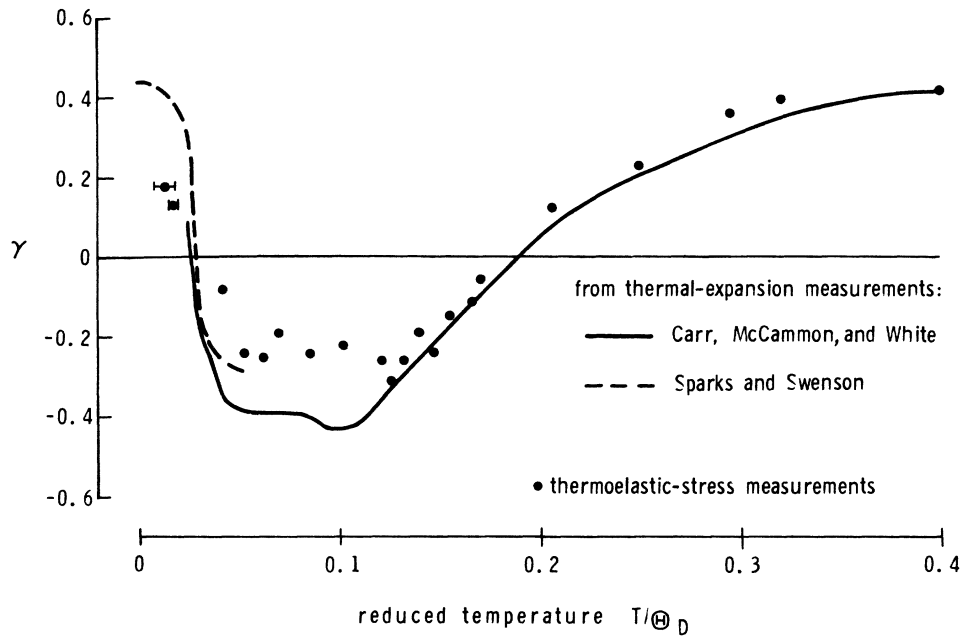


FIG. 3. Gruneisen parameter of silicon as a function of reduced temperature ( $\Theta_D = 645^\circ\text{K}$ ), as measured directly and as calculated from thermal expansion, specific heat, bulk modulus, and density.

sit time through the sample as a function of temperature. The room-temperature sound speed was observed to be  $6.42 \times 10^5$  cm/sec. Using the thermal-expansion data of Clark<sup>25</sup> and the observed shift in the time of arrival of the stress pulse, the velocity at  $77^\circ\text{K}$  is calculated to be  $6.56 \times 10^5$  cm/sec. Comparison can be made with the elastic-constant measurements of Vallin *et al.*<sup>27</sup> on single

crystals of aluminum. The values calculated from those data for the dilational sound velocities in a polycrystalline aggregate are  $6.419 \times 10^5$  cm/sec and  $6.410 \times 10^5$  cm/sec at room temperature by the Voigt and Reuss schemes, respectively. The corresponding values at  $77^\circ\text{K}$  are  $6.575 \times 10^5$  cm/sec and  $6.567 \times 10^5$  cm/sec,<sup>28</sup> in good agreement with the present results.

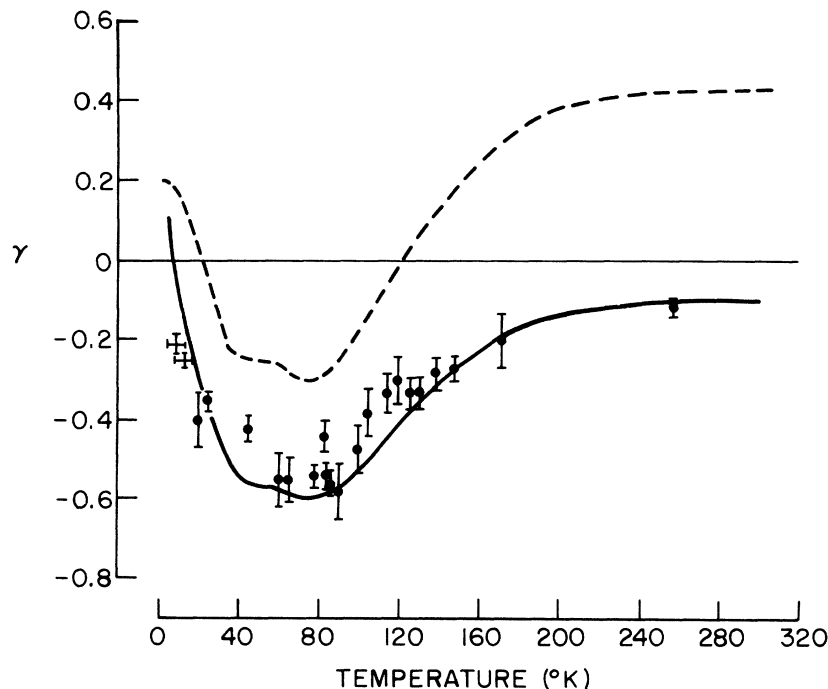


FIG. 4. Gruneisen parameter measured for  $1.5 \times 10^{-3}$  to  $2.5 \times 10^{-3}$   $\Omega$  cm *p*-type silicon (dashed line); and the effective Gruneisen parameter, including the electronic volume effect, for  $10^3$  to  $3 \times 10^3$   $\Omega$  cm silicon as calculated (solid line) and measured (points).

*Silicon.* The low-temperature results for the highly doped silicon sample are shown again in Fig. 3, together with Grüneisen parameters calculated from the thermal-expansion measurements of Carr, McCammon, and White<sup>29</sup> and of Sparks and Swenson.<sup>10</sup> The direct measurements and the thermal-expansion data indicate the same general behavior.

Two quantitative discrepancies are observed, however. First, the present data indicate a smaller absolute value of the minimum than those of Carr *et al.* The values of Sparks and Swenson, although not extended to high-enough temperatures, appear also to level off at a smaller absolute value. Second, if the shape of the Sparks and Swenson curve is assumed to be correct, then the thermoelastic stresses suggest a lower positive limiting value of the Grüneisen parameter. This lower value of about 0.2 agrees with the value of  $0.24 \pm 0.02$  calculated from the pressure derivatives of the elastic constants.<sup>11</sup>

The measurements on high-resistivity silicon were done to check the analysis of the electronic volume effect and to see whether, from a comparison with results on doped silicon, an effect on  $\gamma$ , attributable to doping (in addition to the expected electronic volume effect) would be observed. Figure 4 shows (as a dashed line) the measured Grüneisen parameter for the highly doped sample. The solid line indicates the expected values of an effective Grüneisen parameter for intrinsic material, calculated from Eqs. (12) and (10). The values of the energy gap as a function of temperature were taken from Macfarlane and co-workers.<sup>30</sup> The points are the measured values for the high-resistivity silicon, again with the vertical error bars representing the root-mean-square deviations

and the horizontal bars showing the temperature resolution at the lowest temperatures.

The calculated and measured values agree qualitatively. Within the experimental accuracy there is no effect on the lattice  $\gamma$  attributable to doping.

The change of acoustic transit time with temperature through the silicon samples was too slight to be observed with any accuracy.

*Errors.* The principal sources of error were the reproducibility of the electron pulses and the calibration of the FET preamplifier as a function of temperature. The maximum uncertainty in  $\gamma$  was estimated to be about 25%. The change of the piezoelectric properties of quartz with temperature is slight<sup>31,32</sup> and was not taken into account. Another potential source of error is a gradual failure or improvement of the bond as the temperature is lowered. As stated above, only data from runs without hysteresis, which is usually associated with bond failure and subsequent healing, were retained.

## VI. CONCLUSION

The experiments have demonstrated that the measurement of inertial thermoelastic stresses provides a convenient tool for determining material properties. It is hoped that further refinements, particularly the development of a heating source with better reproducibility, will provide better resolution at low temperatures. It is expected that the technique will be particularly useful for characterizing poorly understood materials, such as polymers and composites.

## ACKNOWLEDGMENT

I thank G. D. Miller for assistance in carrying out the experiments.

<sup>†</sup>Work supported by the U. S. Atomic Energy Commission.

<sup>1</sup>R. A. Graham and R. E. Hutchison, *Appl. Phys. Letters* **11**, 69 (1967).

<sup>2</sup>R. B. Oswald, Jr., D. R. Schallhorn, H. A. Eisen, and F. B. McLean, *Appl. Phys. Letters* **13**, 279 (1968).

<sup>3</sup>R. B. Oswald, Jr., F. B. McLean, D. R. Schallhorn, and L. D. Buxton, *Appl. Phys. Letters* **16**, 24 (1970).

<sup>4</sup>F. C. Perry, *J. Appl. Phys.* **41**, 5017 (1970).

<sup>5</sup>W. B. Gauster, *Phys. Rev.* **187**, 1035 (1969).

<sup>6</sup>For a review, see J. G. Collins and G. K. White, in *Progress in Low Temperature Physics*, edited by C. J. Gorter (North-Holland, Amsterdam, 1964), Vol. 4, p. 450.

<sup>7</sup>K. Andres, *Phys. Kondensierten Materie* **2**, 294 (1964).

<sup>8</sup>D. Bijl and H. Pullan, *Physica* **21**, 285 (1955).

<sup>9</sup>D. B. Fraser and A. C. Hollis Hallett, *Can. J. Phys.* **43**, 193 (1965).

<sup>10</sup>P. W. Sparks and C. A. Swenson, *Phys. Rev.* **163**, 779 (1967).

<sup>11</sup>A. G. Beattie and J. E. Schirber, *Phys. Rev. B* **1**, 1548 (1970).

<sup>12</sup>T. A. Zaker, *J. Appl. Mech.* **32**, 143 (1965).

<sup>13</sup>W. B. Gauster, *J. Mech. Phys. Solids* (to be published).

<sup>14</sup>See, e.g., V. S. Vavilov, *Effects of Radiation on Semiconductors* (Consultants Bureau, New York, 1965), Chap. 3.

<sup>15</sup>W. Shockley, *Solid-State Electron.* **2**, 35 (1961).

<sup>16</sup>F. E. Emery and T. A. Rabson, *Phys. Rev.* **140**, A2089 (1965).

<sup>17</sup>A. R. Beattie and P. T. Landsford, *Proc. Roy. Soc. (London)* **A249**, 16 (1959).

<sup>18</sup>Field Emission Corp., McMinnville, Ore.

<sup>19</sup>Janis Research Co., Inc., Stoneham, Mass.

<sup>20</sup>This technique is mentioned by R. D. Peters, M. A. Breazeale, and V. K. Paré, *Phys. Rev. B* **1**, 3245 (1970). I am indebted to Professor Breazeale for pointing it out to me.

<sup>21</sup>Zenick Associates, Burbank, Calif., Model 421-A2.

<sup>22</sup>W. T. Berg, *Phys. Rev.* **167**, 583 (1968); W. F. Giauque and P. F. Meads, *J. Am. Chem. Soc.* **63**, 1897 (1941).

<sup>23</sup>P. H. Keesom and G. Seidel, *Phys. Rev.* **113**, 33



(1959); P. Flubacher, A. J. Leadbetter, and J. A. Morrison, *Phil. Mag.* **4**, 273 (1959).

<sup>24</sup>D. F. Gibbons, *Phys. Rev.* **112**, 136 (1958).

<sup>25</sup>A. F. Clark, *Cryogenics* **8**, 282 (1968).

<sup>26</sup>For a review, see R. F. Boughton, J. L. Olsen and C. Palmy, in *Progress in Low Temperature Physics*, edited by C. J. Gorter (North-Holland, Amsterdam, 1970), Vol. 6, p. 163.

<sup>27</sup>J. Vallin, M. Mongy, K. Salama, and O. Beckman,

*J. Appl. Phys.* **35**, 1825 (1964).

<sup>28</sup>G. Simmons, *J. Grad. Res. Center* **34**, 157 (1965).

<sup>29</sup>R. H. Carr, R. D. McCammon, and G. K. White, *Phil. Mag.* **12**, 157 (1965).

<sup>30</sup>G. G. Macfarlane, T. P. McLean, J. E. Quarrington, and V. Roberts, *Phys. Rev.* **111**, 1245 (1958).

<sup>31</sup>O. E. Jones, *Rev. Sci. Instr.* **38**, 253 (1967).

<sup>32</sup>A. G. Beda, *Fiz. Tverd. Tela* **9**, 1332 (1967) [*Sov. Phys. Solid State* **9**, 1043 (1967)].

## Calculated Spin-Orbit Splittings of Some Group IV, III-V, and II-VI Semiconductors

G. G. Wepfer, T. C. Collins, and R. N. Euwema

*Aerospace Research Laboratories, Wright-Patterson Air Force Base, Ohio 45433*

(Received 21 December 1970)

The spin-orbit splittings of the valence and conduction bands of the group-IV semiconductors Si, Ge, and  $\alpha$ -Sn, the III-V compounds AlSb, GaP, GaAs, GaSb, InP, InAs, and InSb, and the II-VI compounds ZnS, ZnSe, ZnTe, and CdTe have been obtained at the  $\Gamma$ ,  $X$ , and  $L$  symmetry points in the Brillouin zone. The calculations were made using a relativistic orthogonalized plane wave (ROPW) model. The energies presented are differences in eigenvalues of the Dirac Hamiltonian where the exchange correlation potential operator was approximated by the cube root of the electron density with coefficients suggested by Slater and by Kohn, Sham, and Gaspar (KSG). The calculated values are compared with values obtained from experiments and from previous  $\mathbf{k} \cdot \mathbf{p}$  calculations. The validity of the two-thirds rule for the ratio of the  $L$ -point to  $\Gamma$ -point valence-band spin-orbit splitting is examined. The effects of hydrostatic pressure on the spin-orbit splittings are also presented.

### I. INTRODUCTION

The purpose of this paper is to present calculated crystalline spin-orbit splittings obtained from solutions of the Dirac equation. The Dirac equation is solved using a relativistic orthogonalized-plane-wave (ROPW) formalism with a crystalline potential which is a superposition of isolated-atom potentials.<sup>1,2</sup> This study includes the effect of using a crystalline self-consistent potential and the effect of different exchange approximations upon the calculated splittings. The spin-orbit splittings for a wide variety of semiconductors (Si, Ge,  $\alpha$ -Sn, AlSb, GaP, GaAs, GaSb, InP, InAs, InSb, ZnS, ZnSe, ZnTe, and CdTe) are given in order to check (or establish) trends as well as to give their individual values. Also, the hydrostatic pressure effect upon the spin-orbit splittings is calculated and compared with experiment.

Observations of spin-orbit splittings throughout the Brillouin zone have been made using optical reflectivity,<sup>3</sup> electroreflectance,<sup>4</sup> and absorption<sup>5</sup> spectra. These measurements determine the value of the splittings to within a few hundreds of an eV. In fact the very small increases in the spin-orbit splitting due to hydrostatic pressure have been measured.<sup>6</sup>

On the theoretical side, the spin-orbit splittings

have been calculated using the OPW formalism and first-order perturbation theory by Liu<sup>7</sup> for Si and Ge. Herman *et al.*<sup>8</sup> obtained the valence-band  $\Gamma$ -point splitting by scaling atomic spin-orbit splittings for these compounds. Cardona and co-workers (Ref. 4) have used the  $\mathbf{k} \cdot \mathbf{p}$  perturbation-theory method in which some band information including one or several spin-orbit splittings must be used as input to allow determination of the adjustable parameters. Once these parameters are determined, the band structure throughout the zone can be extrapolated. This works quite well in some cases, but fails at times as will be pointed out later.

The method used in this paper is a "black box" computer program into which the lattice constant and atomic numbers are fed, and out of which comes an unadjusted relativistic band structure. This approach has been utilized by Herman and co-workers<sup>1,2,9</sup> using a relativistic OPW formalism with an isolated-atom crystalline potential and by Eckelt,<sup>10</sup> and Madelung and Treusch<sup>11</sup> who use the Korringa-Kohn-Rostoker (KKR) formalism with a muffin-tin potential derived from a superposition of isolated-atom crystalline potentials.

In Sec. II A, the relativistic OPW formalism is briefly presented. Special attention is given to the insensitivity of the isolated-atom potential model to the shape of the extended tail of the core charge